PHYSICAL REVIEW C VOLUME 59, NUMBER 3 MARCH 1999

Enhancement of $\pi A\to\pi\pi A$ threshold cross sections by in-medium $\pi\pi$ final state interactions

R. Rapp,[1] J. W. Durso,[2,3] Z. Aouissat,[4] G. Chanfray,[5] O. Krehl,[2] P. Schuck,[6] J. Speth,[2] and J. Wambach[4]
[1]*Department of Physics and Astronomy, SUNY at Stony Brook, Stony Brook, New York 11794-3800*
[2]*Physics Department, Mount Holyoke College, South Hadley, Massachusetts 01075*
[3]*Institut für Kernphysik, Forschungszentrum Jülich GmbH, D-52425 Jülich, Germany*
[4]*Institut für Kernphysik, Schloßgartenstrasse 9, TU-Darmstadt, D-64289 Darmstadt, Germany*
[5]*IPN, IN2P3-CNRS/Université Claude Bernard Lyon I, 43 Boulevard du 11 Novembre 1918 F-69622 Villeurbanne Cedex, France*
[6]*ISN, IN2P3-CNRS/Université Joseph Fourier, 53 Avenue de Martyrs, F-38026 Grenoble Cedex, France*

(Received 2 October 1998)

We address the problem of pion production in low-energy π-nucleus collisions. For the production mechanism, we assume a simple model consisting of a coherent sum of single pion exchange and the excitation—followed by the decay into two pions and a nucleon—of the $N^*(1440)$ resonance. The production amplitude is modified by the final state interaction between the pions calculated using the chirally improved Jülich meson exchange model including the polarization of the nuclear medium by the pions. The model reproduces well the experimentally observed $\pi A\to\pi\pi A$ cross sections, especially the enhancement with increasing A of the $\pi^+\pi^-$ mass distribution in the threshold region. [S0556-2813(99)50203-3]

PACS number(s): 25.80.Hp, 13.75.Gx, 13.75.Lb, 21.65.+f

The past ten years have witnessed a considerable increase in our understanding of the $\pi\pi$ interaction. The success of chiral perturbation theory [1,2] in describing the near-threshold behavior of the $\pi\pi$ amplitude is a clear success for the effective field theory approach to the problem. Unfortunately, at energies above a few hundred MeV, where effects of unitarity become important, chiral perturbation theory becomes unwieldy and other approaches must be used to obtain a good description of the free $\pi\pi$ scattering. One such approach is the meson exchange model developed by the Jülich group [3], which gives an excellent quantitative description of $\pi\pi$ and πK scattering phases up to about 1.5 GeV total cm energy. Another is the inverse amplitude method—a variant of the K-matrix approach—of Oset *et al.* [4]. Here we will consider the application of the former to the problem of pion production by pions on nuclei in order to investigate some of the predictions of the model for the behavior of the $\pi\pi$ scattering amplitude in the presence of a nuclear medium. The latest version of this model, which we refer to as the chirally improved Jülich model [5], respects the constraints on the S-wave scattering length imposed by chiral symmetry, while maintaining the quality of fit to the free $\pi\pi$ scattering data. We briefly summarize here the main features of the model and present some of the results of the model for $\pi\pi$ interactions in nuclear matter. For details of the model, we direct the reader to Refs. [5,6].

In the chirally improved Jülich model, the interaction is driven by the exchange of ρ mesons plus contact interactions, as in the Weinberg Lagrangian [7]. This Lagrangian is chirally symmetric in the massless pion limit. The Born approximation for this interaction is used as the potential in a three-dimensional scattering equation of the Blankenbecler-Sugar form [8]. The solution of the scattering equation destroys chiral symmetry through both the partial summation of diagrams and the use of form factors, which are needed to ensure convergence of the integral equation. However, the off-shell behavior of the potential is prescribed in such a way as to preserve the scattering length constraint required by chiral symmetry.

The motivation to ''chirally improve'' the original Jülich model resulted from studies of the behavior of the $\pi\pi$ interaction in nuclear matter as a function of density [9]. In these studies, the polarization of the medium by the pion, principally through the production of nucleon-hole and Δ-hole configurations, significantly reshaped the $\pi\pi$ scattering amplitude. It was observed that models in which the potential term is not chirally symmetric in the limit of zero pion mass led to a rapid increase in attraction between the pions as a function of density, resulting ultimately in spontaneous S-wave pion pair condensation at densities about that of normal nuclear matter. Further studies [10,5,6] showed that the onset of this instability could be shifted to higher densities if the $\pi\pi$ potential term were required to satisfy the low-energy chiral constraints, or if the amplitude calculated from the scattering equation could be forced to obey the same constraints. However, the buildup of attractive strength in the threshold and subthreshold region persisted. In Fig. 1 we show the S-wave $\pi\pi$ scattering amplitudes at low energies in free space and at half nuclear matter density using the chirally improved Jülich model from Ref. [5], which will be employed in the following. Whereas the isospin $I=0$ amplitudes (upper panel) undergo substantial reshaping in the medium, the $I=2$ channel (lower panel) is hardly affected. In the $I=0$ channel, the combination of the attractive $\pi\pi$ interaction and the softening of the in-medium single-pion dispersion relation leads to a substantial accumulation of strength in the imaginary part of the in-medium amplitude (notice, however, that the real part is actually only enhanced for $M_{\pi\pi}\leqslant 300$ MeV). In contrast, the purely repulsive interaction in the $I=2$ channel prevents essential modifications.

Since the in-medium scalar-isoscalar $\pi\pi$ amplitude is the main mediator of the intermediate range attraction in the nucleon-nucleon interaction, it is of prime importance for, e.g., nuclear saturation. In fact, in Refs. [11,12] the use of the chirally improved Jülich model in the Bonn potential for the NN interaction [13] has been shown to be compatible with the empirical nuclear saturation point once medium modifi-

 ©1999 The American Physical Society

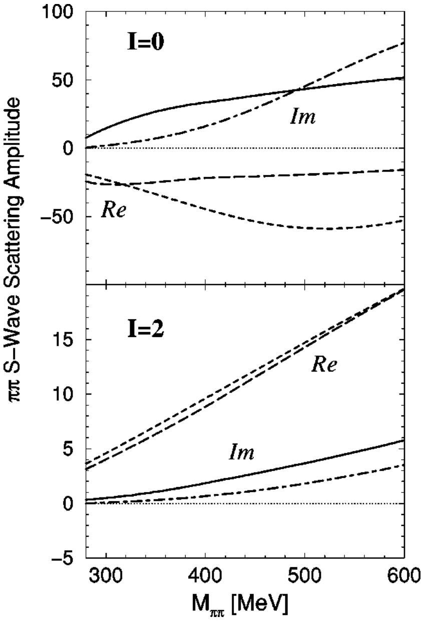

FIG. 1. Dimensionless S-wave $\pi\pi$ scattering amplitudes for total isospin 0 (upper panel) and 2 (lower panel); the short-dashed and dashed-dotted lines correspond to the real and imaginary parts, respectively, in free space, and the long-dashed and full lines correspond to the real and imaginary parts, respectively, at a nuclear density of $\rho=0.5\rho_0$.

cations in the vector mesons exchanges (providing short-range repulsion) are also included. Here we are interested in a more direct assessment of the in-medium $\pi\pi$ S-wave correlations.

A challenging testbed for the in-medium modifications of the two-pion interaction discussed above has been set by recent experimental data taken by the CHAOS Collaboration [14,15] at TRIUMF. An incoming pion beam of nominal kinetic energy $T_\pi=282.7$ MeV was directed at various nuclear targets, and two outgoing pions were detected in coincidence. With increasing nuclear mass number, the corresponding invariant mass spectra show a strong enhancement of $\pi^+\pi^-$ pairs just above the two-pion threshold of $M_{\pi\pi}=2m_\pi$, whereas only very minor variations are observed for $\pi^+\pi^+$ pairs.

That the $\pi^+\pi^-$ strength in the scalar-isoscalar channel in a nuclear medium can be strongly enhanced at threshold was predicted in Ref. [16], based on inclusive data from the CHAOS Collaboration [17]. A first indication that this threshold enhancement can account for the measured $(\pi^+,\pi^+\pi^-)$ cross section at low invariant mass was obtained from a schematic calculation in Ref. [18]. A clue to the possible underlying mechanism for this dramatic effect is provided by the isospin decomposition of the charged states. For S-waves one has

$$\mathcal{M}_{\pi^+\pi^-}=\tfrac{2}{3}\mathcal{M}^{I=0}+\tfrac{1}{3}\mathcal{M}^{I=2}$$

$$\mathcal{M}_{\pi^+\pi^+}=\mathcal{M}^{I=2}, \tag{1}$$

showing that while the $\pi^+\pi^+$ channel is pure isotensor, the $\pi^+\pi^-$ channel is predominantly isoscalar. Thus, the in-medium $\pi\pi$ amplitudes [5] shown in Fig. 1 clearly exhibit desirable features: little modification of the scalar-isotensor amplitude, and a significant low-energy enhancement of the scalar-isoscalar amplitude. To quantify the comparison, the actual cross sections for the $\pi A\to\pi\pi A$ production process must be calculated, including the experimental acceptance of the CHAOS spectrometer, which is crucial to reproducing the precise shapes of the observed spectra.

Since our emphasis here is on possible medium effects in the $\pi\pi$ interaction, we will treat the pion production process in a simplified manner. First, we assume that it always proceeds as an elementary process on a single nucleon. Second, we account only for the two most important contributions which, according to Refs. [19,15], are the one-pion exchange (OPE) reaction (contributing to both isoscalar and isotensor channel) and the $N^*(1440)$ resonance formation (leading to isoscalar $\pi\pi$ states only).

Let us first discuss the OPE contribution. The corresponding 4-differential cross section is given by

$$\frac{d^4\sigma^{\rm OPE}_{\pi N\to\pi\pi N}}{dM_{\pi\pi}dtd\cos\theta_{\rm c.m.}d\phi_{\rm c.m.}} = \frac{M^2_{\pi\pi}}{16\pi^2 p^2_{\rm lab}}\frac{IFf^2_{\pi NN}}{4\pi m^2_\pi}|t|\frac{|\mathcal{M}_{\pi\pi}(M_{\pi\pi},q,q',\cos\theta_{\rm c.m.})|^2}{32\pi M^2_{\pi\pi}} \times q' D_\pi(t)^2, \tag{2}$$

where $M_{\pi\pi}$ is the two-pion invariant mass, $D_\pi(t)=[t-m_\pi^2]^{-1}$ the propagator of the exchanged pion, $p_{\rm lab}$ the incoming pion laboratory momentum, and $q,q',\phi_{\rm c.m.},\theta_{\rm c.m.}$ the in/outgoing pion momentum and their relative angles in the two-pion c.m.s. ($f_{\pi NN}=1.01$ and $IF=2$ for charged pion exchange). Azimuthal symmetry in the $\pi\pi$ interaction makes the $\phi_{\rm c.m.}$ integration trivial. Furthermore, since our focus will be on the near threshold region, the S-wave contribution is expected to be dominant. This is supported by experimental angular distributions in $\cos\theta_{\rm c.m.}$ which do not show any trace of other than (isotropic) S-wave components [14]. We will thus neglect P- and higher partial waves. The invariant mass spectra are then given by

$$\frac{d\sigma^{\rm OPE}}{dM_{\pi\pi}}=4\pi\int_{t_{\rm min}}^{t_{\rm max}}dt\,\frac{d^2\sigma^{\rm OPE}_{\pi N\to\pi\pi N}}{dM_{\pi\pi}dt}{\rm Acc}(t,M_{\pi\pi},s_{\rm tot}). \tag{3}$$

For a meaningful comparison with the experimental spectra, it is essential to include the acceptance of the CHAOS spectrometer, represented by an ''acceptance factor'' ${\rm Acc}(t,M_{\pi\pi},s_{\rm tot})$ in Eq. (3). We evaluate it by Monte Carlo techniques: in the two-pion c.m.s. we randomly generate pairs of angles $(\phi_{\rm c.m.},\cos\theta_{\rm c.m.})$, uniformly distributed over the sphere due to the S-wave nature of the $\pi\pi$ amplitude. (To include higher partial waves, one would need to weight the polar angles with the corresponding angular distribution obtained from the total amplitude for the particular $M_{\pi\pi},q,q'$.) For given $t,M_{\pi\pi},s_{\rm tot}$, one can then determine the total momentum $\vec{P}$ of the pion pair in the laboratory frame and apply the corresponding Lorentz boost to transform the two generated tracks into the lab system. In the latter, the experimental acceptance cuts can then be readily applied, i.e., $\Phi_{\pi\pi}=0°\pm7$ or $\Phi_{\pi\pi}=180°\pm7$ for the out-of-reaction plane opening angle of the pion pair and $\Theta_{\pi^\pm}$

$=10°-170°$ for the in-plane angle of both single pion tracks accounting for the dead regions around the beam direction. At fixed $t, M_{\pi\pi}$ and $s_{\rm tot}$ the acceptance probability is then determined as $\mathrm{Acc}=N_{\rm acc}/N_{\rm tot}$, with $N_{\rm tot}$ the number of trials and $N_{\rm acc}$ the number of events that fall into the experimental acceptance.

In order to assess the $N^*(1440)$ contribution, we model the two-pion production amplitude as proceeding via an intermediate scalar-isoscalar resonance $\tilde{\sigma}$ of invariant mass $M_{\pi\pi}$, which subsequently decays into two pions, i.e., $\pi N \rightarrow N^*(1440) \rightarrow \tilde{\sigma} N \rightarrow \pi\pi N$. Since in the Jülich model, there is no low-lying genuine σ resonance [the "$\sigma(550)$" being chiefly generated through attractive t-channel ρ exchange, and the $f_0(980)$ being realized as a $K\bar{K}$ bound state], we identify the $\tilde{\sigma}$ with the ϵ resonance located at around $M_{\pi\pi} \simeq 1400$ MeV. Its coupling to $\pi\pi$ states is well determined by a satisfactory fit to the $\delta^{00}_{\pi\pi}$ phase shifts above 1 GeV [5]. For the $N^*(1440)N\epsilon$ vertex, we assume scalar coupling,

$$\mathcal{L}_{N^*N\epsilon}=g_{N^*N\epsilon}\Psi^\dagger_{N^*}\epsilon\Psi_N+\mathrm{H.c.} \tag{4}$$

and estimate the corresponding coupling constant $g_{N^*N\epsilon}$ from the experimentally measured branching ratio of 5–10% for $N^*(1440)\rightarrow N(\pi\pi)^{I=0}_{S-\mathrm{wave}}$ [20]. Similarly, for the entrance channel, we employ the usual interaction vertex

$$\mathcal{L}_{N^*N\pi}=\frac{f_{N^*N\pi}}{m_\pi}\Psi^\dagger_{N^*}\vec{\sigma}\cdot\vec{q}\,\tau_a\pi_a\Psi_N+\mathrm{H.c.}, \tag{5}$$

and adjust the $N^*N\pi$ coupling constant to the branching ratio for $N^*(1440)\rightarrow N\pi$ of 60–70% [20]. In Born approximation, the cross section for $\pi N \rightarrow N^*(1440) \rightarrow \epsilon N$ with an ϵ of invariant mass $M_{\pi\pi}$ and 3-momentum P is then obtained as

$$\sigma_{\pi N\rightarrow N^*\rightarrow\epsilon N}(s_{\rm tot},M_{\pi\pi})=\frac{\overline{|\mathcal{M}_{N^*\epsilon}|^2}M_N}{8\pi p^2_{\rm lab}}\int_{P_{\rm min}}^{P_{\rm max}}dP\,\frac{P}{E_\epsilon(P)} \tag{6}$$

with the spin averaged invariant matrix element in the πN c.m.s.

$$\overline{|\mathcal{M}_{N^*\epsilon}|^2}=\frac{IF}{2}\,\frac{f^2_{N^*N\pi}}{m^2_\pi}g^2_{N^*N\epsilon}\frac{q^2_{\rm in}}{|\sqrt{s_{\rm tot}}-M_{N^*}-\mathrm{i}\Gamma_{N^*}/2|^2}. \tag{7}$$

The decay of the ϵ is now included by folding the cross-section Eq. (6) over the fully dressed ϵ spectral function which automatically accounts for the final state interaction of the pion pair [10]:

$$\sigma_{\pi N\rightarrow N^*\rightarrow\pi\pi N}(s_{\rm tot})=\int\frac{dM_{\pi\pi}M_{\pi\pi}}{\pi}A_\epsilon(M_{\pi\pi})\sigma_{\pi N\rightarrow N^*\rightarrow\epsilon N}(s_{\rm tot},M_{\pi\pi}). \tag{8}$$

with

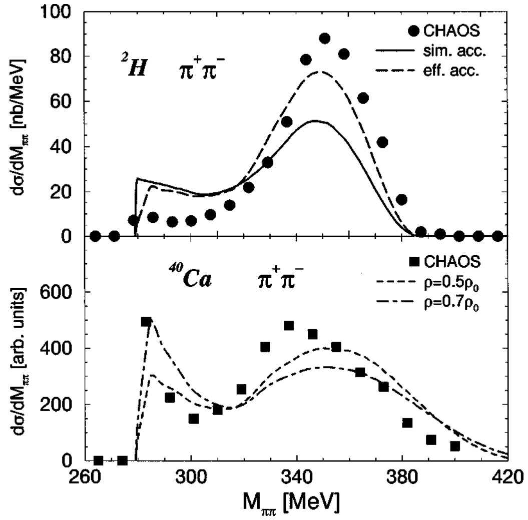

FIG. 2. Results for pion production cross sections in the $\pi^+\pi^-$ channel using the chirally improved Jülich $\pi\pi$ interaction from Ref. [5]; upper panel: on the deuteron target using the Monte Carlo–simulated acceptance (full lines) and the parameterized, "effective" acceptance; lower panel: on Calcium, using the effective acceptance, for two different densities. The ^{2}H and ^{40}Ca data are from Refs. [15] and [14], respectively.

$$A_\epsilon(M_{\pi\pi})=[D^0_\epsilon(M_{\pi\pi})]^2\pi v^2_{\epsilon\pi\pi}q'M_{\pi\pi}\times[1-\pi q'M_{\pi\pi}\mathrm{Im}\mathcal{M}^{00}_{\pi\pi}(M_{\pi\pi})], \tag{9}$$

where $v_{\epsilon\pi\pi}$ denotes the $\epsilon\pi\pi$ vertex function and $\mathcal{M}^{00}_{\pi\pi}$ the full $\pi\pi$ scattering amplitude in the $JI=00$ channel. After a variable transformation, $dP=E_\epsilon(P)/(2M_NP)dt$, and inclusion of the experimental acceptance, we finally obtain the differential mass spectrum

$$\frac{d\sigma^{N^*}}{dM_{\pi\pi}}=\frac{\overline{|\mathcal{M}_{N^*\epsilon}|^2M_{\pi\pi}A_\epsilon(M_{\pi\pi})}}{16\pi^2p^2_{\rm lab}}\int_{t_{\rm min}}^{t_{\rm max}}dt\,\mathrm{Acc}(t,M_{\pi\pi},s_{\rm tot}). \tag{10}$$

The cross section we wish to calculate requires a coherent sum of the OPE and $N^*(1440)$ *amplitudes*. The result of this yields the $M_{\pi\pi}$ differential cross section

$$\frac{d\sigma^{\mathrm{OPE}+N^*}}{dM_{\pi\pi}}=\frac{q'}{16\pi^3p^2_{\rm lab}}\times\int_{t_{\rm min}}^{t_{\rm max}}dt\,\mathrm{Acc}(t,M_{\pi\pi},s_{\rm tot})|\mathcal{M}^{\rm OPE}+\mathcal{M}^{N^*}|^2, \tag{11}$$

where the amplitudes $\mathcal{M}^{\rm OPE}$ and $\mathcal{M}^{N^*}$ can be read off by comparison with Eqs. (3) and (10), respectively.

In the upper panels of Figs. 2 and 3 our results for deuterium target are displayed. The cross sections are calculated in absolute units using the free $\pi\pi$ interaction. The full lines correspond to a calculation with the Monte Carlo–simulated acceptance as described above. In the $\pi^+\pi^-$ channel, the theoretical curves somewhat overestimate the data for $M_{\pi\pi} \leqslant 320$ MeV, and underestimate them for $M_{\pi\pi} \geqslant 350$ MeV, a feature that is also shared by the model cal-

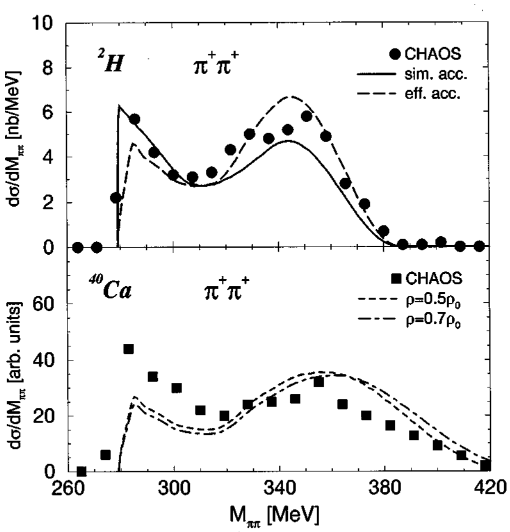

FIG. 3. Results for pion production cross sections in the $\pi^+\pi^+$ channel using the chirally improved Jülich $\pi\pi$ interaction; identical line identification as in Fig. 2.

culations shown in Ref. [15]; in the $\pi^+\pi^+$ channel, the agreement is quite satisfactory. To check our determination of the experimental acceptance, we also performed calculations with an ''effective acceptance'' (dashed lines in the upper panels); this was extracted from a fit to a phase space simulation given in Ref. [15], which, after dividing out the phase space, leads to a simple $M_{\pi\pi}$-dependent acceptance factor Acc($M_{\pi\pi}$). Whereas the description of the $\pi^+\pi^-$ channel turns out to be somewhat improved, the opposite trend is found in the $\pi^+\pi^+$ channel. In general, both ways of implementing the experimental acceptance agree reasonably well—within 20 percent.

When moving to finite nuclei, the effect of the nuclear Fermi motion has to be included. In principle this is very complicated, even if everything about the location of the interaction within the nucleus were known. We adopt instead a simplified procedure that, as we will see, can adequately account for the observed cross sections. First, we assume that the production of the pion pairs occurs at a definite density. In principle one should then average over all momenta within the Fermi sphere for that density, which would mean calculating the cross section for noncollinear collisions, and we should also account for the effective mass of the nucleon as a function of momentum. This is computationally tedious and, given the precision of the data, largely unnecessary. One can show that sufficient accuracy—on the order of one percent or better—is obtained if the average is performed only over the component of the nucleon momentum along the beam direction. In this case one has

$$\left(\frac{d\sigma^{\mathrm{OPE}+N^*}}{dM_{\pi\pi}}\right)_{\mathrm{av}}=\frac{3}{4k_F^3}\int_{-k_F}^{+k_F}dk_z(k_F^2-k_z^2)\frac{d\sigma^{\mathrm{OPE}+N^*}}{dM_{\pi\pi}}[s_{\mathrm{tot}}(k_z)], \tag{12}$$

with $s_{\mathrm{tot}}(k_z)=m_\pi^2+M_N^2+2[\omega_{p_{\mathrm{lab}}}E_N(k_z)-p_{\mathrm{lab}}k_z]$ and the Fermi momentum given in terms of the local density by $\rho_N=2k_F^3/3\pi^2$. (In fact, we adopted the same procedure for the deuteron calculations with an ''effective'' Fermi momentum representing the kinematical limit where the two nucleons recoil together.)

Of course pions undergo substantial absorption in the nuclear medium—an effect which, as implied in the previous paragraph, we did not include in the present analysis. Here we address instead the question of whether the medium modifications of the final state $\pi\pi$ interaction can account for the dramatic reshaping of the mass distribution observed in the CHAOS experiment. To fix the units for the in-medium results, we assume that our theoretical total cross sections account for the same fraction of the measured cross sections as on the ^2H target (note again that our deuteron results are in absolute units), which ranges between 80% and $\sim 100\%$. The use of the in-medium $\pi\pi$ amplitudes in the differential cross sections then leads to the results shown in the lower panel of Figs. 2 and 3, where we have employed the parameterized, ''effective'' experimental acceptance.

In the $\pi^+\pi^+$ channel, the density dependence is very weak, the major effect being a smearing of the cross section due to the nuclear Fermi motion. However the $\pi^+\pi^-$ channel exhibits very substantial medium effects; in particular, the strong threshold enhancement observed in the data is nicely accounted for by our model, being entirely due to the effects in the in-medium isoscalar *S*-wave $\pi\pi$ amplitude $\mathcal{M}_{\pi\pi}^{00}$. The average nuclear density which seems to reproduce the ^{40}Ca data best turns out to be slightly above half the saturation density ($\rho=0.5$–$0.7\rho_0$). This is in line with the average density of ^{40}Ca and the fact that the two pions are probably created near the surface. One should, however, realize that the two outgoing pions are at rather low energies and can therefore pass the nucleus with little attenuation. Also note that the ratio of the threshold peak to the main maximum at $M_{\pi\pi}\simeq 350$ MeV increases within rather small increases of density, a trend that is also clearly seen in the experimental data when going to heavier nuclei (from ^{12}C to ^{40}Ca to ^{208}Pb) [15], where one would expect to probe slightly increasing average densities.

To summarize, we have analyzed $A(\pi^+,\pi^+\pi^\pm)$ production cross sections on the deuteron and nuclei at low energies using a realistic model of the $\pi\pi$ interaction which accurately describes free $\pi\pi$ scattering over a wide range of energies and incorporates ''minimal chiral constraints.'' Our emphasis was on the *S*-wave $\pi\pi$ final state interaction and, in particular, its modifications by the medium. The latter were included in terms of the standard renormalization of pion propagation through nucleon/Δ-hole excitations entering a Lippmann-Schwinger-type equation for the $\pi\pi$ amplitude. Many aspects of the complicated reaction dynamics have been treated approximately—e.g., the pion production process, the nuclear Fermi motion and absorption—or neglected altogether—e.g., Coulomb interactions and the dependence of the medium corrections on the total two-pion 3-momentum. Nevertheless, we find that our calculations, including experimental acceptance, agree reasonably well with recent data taken by the CHAOS Collaboration at TRIUMF in both the $\pi^+\pi^-$ and the $\pi^+\pi^+$ channel. In particular, the strong enhancement of the $\pi^+\pi^-$ cross section very close to the free two-pion threshold can be well reproduced by ascribing it to the medium-modified scalar-isoscalar $\pi\pi$ interaction. Such an enhancement is absent in the isotensor $\pi^+\pi^+$ interaction, which is also consistent with the data. The physical origin of these features is rather simple: the softening of the in-medium single-pion dispersion relation acts coherently with the attractive interaction in the isoscalar channel, but is not effective in the purely repulsive isotensor channel.

The outgoing two pions being on-mass-shell precludes any statement as to whether the threshold enhancement of the in-medium isoscalar $\pi\pi$ amplitude entails substantial subthreshold effects at higher densities, as predicted in various $\pi\pi$ models. However, since the $\pi^+\pi^-$ correlations in the $J=I=0$ channel are of great importance for the understanding of nuclear binding, further experimental and theoretical studies of the subject will certainly be of great interest.

Useful discussions with N. Grion are gratefully acknowledged. Two of us (JWD and RR) wish to thank Professor J. Speth for his hospitality and support during their visits to the Forschungszentrum Jülich. One of us (R.R.) acknowledges support from the Alexander-von-Humboldt foundation as a Feodor-Lynen fellow, and also thanks Professor J. Wambach for his hospitality and support during the visits to TU Darmstadt. This work was supported in part by the U.S. Department of Energy under Grant No. DE-FG02-88ER40388.

[1] J. Gasser and H. Leutwyler, Nucl. Phys. **B250**, 465 (1985).
[2] J. F. Donoghue, C. Ramirez, and G. Valencia, Phys. Rev. D **38**, 2195 (1988).
[3] D. Lohse, J. W. Durso, K. Holinde, and J. Speth, Phys. Lett. B **234**, 235 (1989); Nucl. Phys. **A516**, 513 (1990); B. C. Pearce, K. Holinde, and J. Speth, *ibid.* **A541**, 663 (1992); G. Janssen, B. C. Pearce, K. Holinde, and J. Speth, Phys. Rev. D **52**, 2690 (1995).
[4] J. A. Oller and E. Oset, Nucl. Phys. **A620**, 438 (1997).
[5] R. Rapp, J. W. Durso, and J. Wambach, Nucl. Phys. **A596**, 436 (1996).
[6] R. Rapp, Ph.D. thesis, Bonn, 1996, in *Berichte des Forschungszentrum Jülich* 3195 (Jülich, 1996).
[7] S. Weinberg, Phys. Rev. Lett. **17**, 616 (1966); Phys. Rev. **166**, 1568 (1968).
[8] R. Blankenbecler and R. Sugar, Phys. Rev. **142**, 1051 (1966).
[9] G. Chanfray, Z. Aouissat, P. Schuck, and W. Nörenberg, Phys. Lett. B **256**, 325 (1991); V. Mull, J. Wambach, and J. Speth, *ibid.* **286**, 13 (1992); Z. Aouissat, G. Chanfray, and P. Schuck, Mod. Phys. Lett. A **15**, 1379 (1993).
[10] Z. Aouissat, R. Rapp, G. Chanfray, P. Schuck, and J. Wambach, Nucl. Phys. **A581**, 471 (1995).
[11] R. Rapp, J. W. Durso, and J. Wambach, Nucl. Phys. **A615**, 501 (1997).
[12] R. Rapp, R. Machleidt, J. W. Durso, and G. E. Brown, Report No. SUNY-NTG-97-22, nucl-th/9706006.
[13] R. Machleidt, K. Holinde, and Ch. Elster, Phys. Rep. **149**, 1 (1987).
[14] CHAOS Collaboration, F. Bonutti *et al.*, Phys. Rev. Lett. **77**, 603 (1996).
[15] F. Bonutti *et al.*, Nucl. Phys. **A638**, 729 (1998).
[16] P. Schuck, W. Nörenberg, and G. Chanfray, Z. Phys. A **330**, 119 (1988).
[17] N. Grion *et al.*, Phys. Rev. Lett. **59**, 1080 (1987).
[18] P. Schuck *et al.*, Proceedings of the XXXVI International Winter Meeting on Nuclear Physics, Bormio, Italy, 1988, edited by I. Iori, nucl-th/9806069.
[19] E. Oset and M. J. Vicente-Vacas, Nucl. Phys. **A446**, 584 (1985).
[20] Particle Data Group, R. Barnett *et al.*, Phys. Rev. D **54**, 1 (1996).